

# MaDiS: Taming Masked Diffusion Language Models for Sign Language Generation

Ronglai Zuo    Rolandos Alexandros Potamias    Qi Sun    Evangelos Ververas  
 Jiankang Deng    Stefanos Zafeiriou  
 Imperial College London

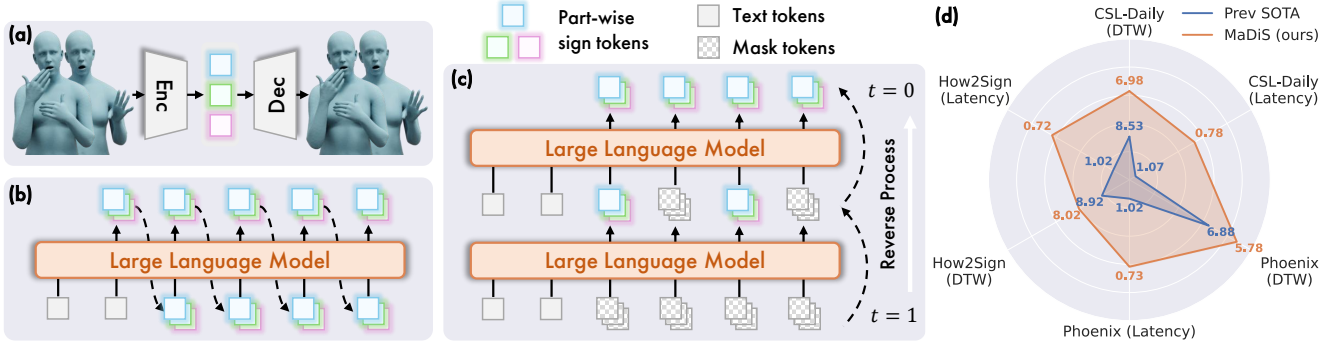


Figure 1. We propose MaDiS, a novel sign language generation approach built upon masked diffusion language models (MDLMs) [45]. (a) A sign tokenizer discretizes continuous sign motions into part-wise tokens [98]. (b) Conventional autoregressive language models generate tokens in a left-to-right manner, limiting utilization of contexts and inference efficiency. (c) The emerging MDLMs model token distributions with bidirectional contexts and enable parallel multi-token sampling during inference. (d) MaDiS achieves SOTA performance across multiple benchmarks [11, 18, 94] while reducing inference latency by nearly 30%.

## Abstract

Sign language generation (SLG) aims to translate written texts into expressive sign motions, bridging communication barriers for the Deaf and Hard-of-Hearing communities. Recent studies formulate SLG within the language modeling framework using autoregressive language models, which suffer from unidirectional context modeling and slow token-by-token inference. To address these limitations, we present MaDiS, a masked-diffusion-based language model for SLG that captures bidirectional dependencies and supports efficient parallel multi-token generation. We further introduce a tri-level cross-modal pretraining scheme that jointly learns from token-, latent-, and 3D physical-space objectives, leading to richer and more grounded sign representations. To accelerate model convergence in the finetuning stage, we design a novel unmasking strategy with temporal checkpoints, reducing the combinatorial complexity of unmasking orders by over  $10^{41}$  times. In addition, a mixture-of-parts embedding layer is developed to effectively fuse information stored in different part-wise sign tokens through learnable gates and well-optimized codebooks. Extensive experiments on CSL-Daily, Phoenix-2014T, and How2Sign demonstrate that MaDiS achieves superior performance across multiple metrics, including DTW error and

two newly introduced metrics, SiBLEU and SiCLIP, while reducing inference latency by nearly 30%. Code and models will be released on our [project page](#).

## 1. Introduction

Sign language is the primary communication mode for Deaf and Hard-of-Hearing (DHH) individuals, yet in predominantly oral societies they are often encouraged to rely on text instead of their preferred sign language [85]. Research in sign language translation (SLT, sign-to-text) and generation (SLG, text-to-sign) aims to improve the accessibility of sign language, thereby mitigating the communication gap between the hearing and DHH communities. While SLT has seen significant progress [14, 21, 23, 28, 31, 37, 46, 76, 97], SLG remains relatively underexplored.

Typical SLG works [5, 19, 64, 68, 73] formulate the task as a visual content generation problem, using either GANs [61] or diffusion models [56]. Recently, motivated by the linguistic character of sign language and the generalizability of large language models (LLMs), a new research direction has emerged that models SLG through tokenization (Figure 1a) and autoregressive language models (ARLMs) [17, 20, 84, 87, 98] (Figure 1b). However, ARLMs have two main limitations: their left-to-right generation order restricts the use of bidirectional contexts and their one-token-

at-a-time decoding introduces an inference bottleneck.

To address such problems, we propose MaDiS (Figure 1c), a novel SLG approach built upon an emerging and promising language modeling paradigm, the masked diffusion language model (MDLM) [44, 45, 82, 86]. Unlike conventional ARLMs, MDLMs are based on masked diffusion models [47, 58, 62], which introduce a forward data masking process and train a mask predictor to approximate the reverse denoising process. This mechanism enables MDLMs to construct model distributions with bidirectional dependencies, allowing them to capture richer contextual information. During the reverse process, multiple tokens can be sampled simultaneously, thereby improving inference efficiency.

Pretraining plays a crucial role in sign language understanding models [29, 34, 37, 77, 92, 95], yet pretraining for SLG models remains largely unexplored. MDLMs are typically pretrained in the token space using a mask-then-predict framework [45], where a subset of tokens is randomly masked and subsequently predicted by the model. Although such token-space objective is well-established in natural language processing, recent advances in self-supervised learning [4, 6, 36] have demonstrated that latent-space pretraining is often more effective in a wide range of vision tasks, including image and video understanding [6, 43] and world modeling [3, 93]. Moreover, sign language, as a visual language, conveys most of its semantics through body and hand motions in the 3D physical space. Motivated by the advantages of different representation spaces, we propose a tri-level cross-modal pretraining method in which the model learns to predict masked text and sign tokens, latent features, and 3D sign motions simultaneously. This challenging and comprehensive pretraining objective encourages the model to learn rich and grounded sign representations and yields significant performance improvements in the downstream SLG task.

After pretraining, we perform supervised fine-tuning conditioned on unmasked text tokens. The original MDLM can be viewed as an any-order ARLM [65]. Due to its unconstrained confidence-based unmasking strategy, the number of possible unmasking orders is enormous. For example, generating 100 tokens in 25 steps results in approximately  $10^{123}$  possible orders. Although this property enables MDLMs to perform well in data-constrained scenarios, it also leads to significantly slower convergence, often requiring more training epochs [52]. To address this issue, we propose a novel unmasking strategy with temporal checkpoints. Inspired by the effectiveness of VAR [70], which generates images progressively from low to high resolution, we insert checkpoints at noise levels 0.75 and 0.5, corresponding to temporal resolutions of  $T/4$  and  $T/2$ . This design dramatically prunes unmasking orders by over  $10^{41}$  times, thereby accelerating convergence dur-

ing training. Furthermore, to better integrate part-wise sign tokens [98], we propose a plug-and-play mixture-of-parts (MoP) embedding layer. Unlike the previous SOTA method [98] that simply averages token embeddings from different body parts, our MoP embedding layer is built upon well-optimized VQ-VAE codebooks, and part-wise embeddings are dynamically fused through learnable gates. In summary, our contributions are as follows:

- We propose MaDiS, a novel SLG approach built upon MDLMs that enable bidirectional context modeling and parallel multi-token generation.
- A tri-level cross-modal pretraining framework is developed that jointly learns from token, latent, and 3D physical spaces, enabling the model to learn richer and more grounded sign representations.
- To accelerate training convergence, we design a novel token unmasking strategy with temporal checkpoints, which significantly reduces unmasking order complexity. To enhance the integration of part-wise sign tokens, we introduce an MoP embedding layer that is conditioned on VQ-VAE codebooks and controlled by learnable gates.
- Extensive experiments on widely adopted benchmarks [11, 18, 94] demonstrate that MaDiS achieves SOTA performance across multiple metrics, including DTW error and two newly introduced metrics, SiBLEU and SiCLIP, while reducing inference latency by  $\sim 30\%$  (Figure 1d).

## 2. Related Work

**Sign Language Generation (SLG).** SLG aims to translate texts into sign language outputs represented in various forms, such as skeletons [1, 60, 67, 68, 79], RGB videos [53, 61, 73], and 3D motions [54, 84, 96, 98]. Although real-person videos are more realistic, developing end-to-end sign video generation models is challenging due to the high dimensionality of RGB video data. Therefore, we focus on generating sign motions, which can serve as an intermediate representation for subsequent sign video synthesis [63, 64]. Motivated by the linguistic nature of sign language, recent studies [17, 84, 87, 98] formulate SLG within a language modeling framework. However, these approaches rely on ARLMs, which are inherently limited by their left-to-right generation process. In this work, we explore emerging MDLMs for SLG, which model token distributions bidirectionally and enable efficient parallel generation.

**Masked Diffusion Language Model (MDLM).** Current LLMs are mostly built upon ARLMs. Although ARLMs demonstrate strong capability, their left-to-right generation order limits both efficiency and context modeling. Recently, MDLMs [24, 44, 45] have emerged as a new language modeling paradigm, showing promising capability and scalability, even surpassing ARLMs on the reversal poem completion task. MDLMs have also been successfully applied to diverse domains, including multimodal understanding [82],

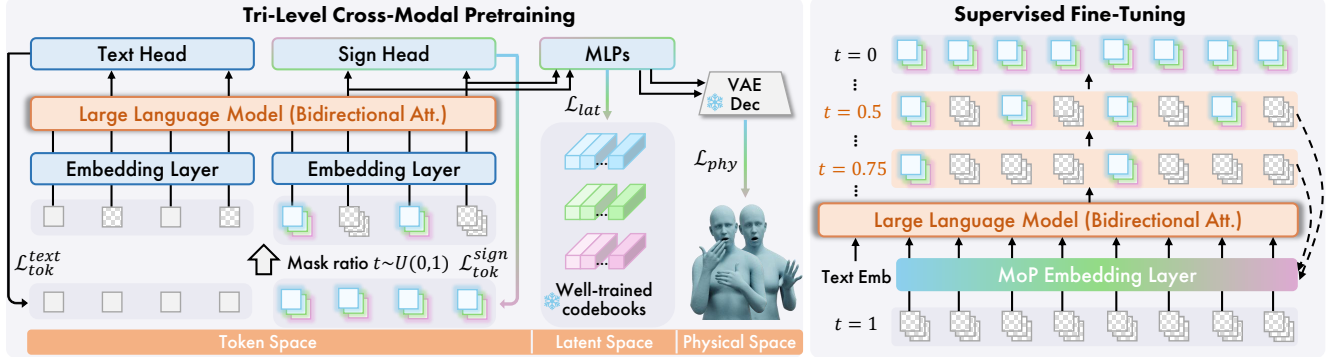


Figure 2. MaDiS is built upon the emerging masked diffusion language model (MDLM), implemented by modifying a standard decoder-only LLM with bidirectional attention. The MDLM is first pretrained with three objectives ( $\mathcal{L}_{tok}^{text} + \mathcal{L}_{tok}^{sign}$ ,  $\mathcal{L}_{lat}$ ,  $\mathcal{L}_{phy}$ ) from the token, latent, and 3D physical spaces, respectively. We then fine-tune the model conditioned on text inputs using the proposed temporal-checkpoint unmasking strategy and a dedicated mixture-of-parts sign embedding layer.

protein design [74], and robotics [75]. A related line of work in human motion generation [26, 27, 51] adopts a similar masked generation approach [12], but their training objectives are determined heuristically and lack the rigorous theoretical foundation of MDLMs. In this work, we present the first effort to introduce MDLMs into SLG and propose a temporal-checkpoint unmasking strategy to improve training efficiency of MDLMs [52].

**Pretraining for Sign Language Models.** Pretraining plays a crucial role in sign language understanding tasks such as recognition and translation. Existing works can be categorized into alignment-based methods [15, 34, 35, 83, 92], which pretrain by aligning signs and texts; reconstruction-based methods [25, 29, 57, 77, 90, 91], which pretrain by reconstructing sign inputs; hybrid methods [95]; and next-token prediction methods [37, 88]. However, an important oversight is that all these works focus solely on understanding tasks. Our work represents the first attempt to pretrain sign language generation models through a cross-modal and multi-level strategy that jointly predicts sign and text tokens, latent features, and 3D sign motions, thereby effectively injecting sign-aware knowledge into MDLMs.

### 3. Methodology

An overview of the proposed MaDiS is illustrated in Figure 2. In the first stage, both text and sign tokens are randomly masked according to a masking ratio  $t$ , and the MDLM is pretrained with objectives defined across multiple representation spaces (token, latent, and physical) to exploit the benefits from multi-level sign representations. In the subsequent fine-tuning stage, the MDLM keeps text tokens unmasked and learns to generate sign tokens using the proposed unmasking with temporal checkpoints (UTC) strategy and the mixture-of-parts (MoP) embedding layer.

### 3.1. Preliminaries

**Sign Tokenizer.** We adopt the open-sourced SOTA decoupled tokenizer [98] to convert continuous sign motions into discrete tokens. It consists of three parallel VQ-VAEs [72] responsible for different body parts. Each VQ-VAE includes an encoder  $\mathcal{E}_p$ , a decoder  $\mathcal{D}_p$ , and a codebook  $\mathcal{C}_p = \{\mathbf{c}_p^i\}_{i=1}^{N_c}$ , where  $p \in \{b, l, r\}$  represents the upper body, left hand, and right hand, respectively, and  $N_c$  is the codebook size. Using this tokenizer, a  $T$ -frame sign motion sequence  $\mathbf{S} \in \mathbb{R}^{T \times d_s}$ , where  $d_s = 133$  denotes the number of SMPL-X parameters [49], is decomposed as three part-wise token sequences  $x_p = \{x_p^i\}_{i=1}^{L_s}$ , where  $x_p^i \in \{1, \dots, N_c\}$  and  $L_s$  denotes the token sequence length.

**Masked Diffusion Language Model.** MDLMs [44, 45, 82] introduce a new language modeling paradigm based on a forward-reverse discrete diffusion process. In the forward process, the original token sequence  $x_0$  is corrupted with mask tokens  $|\mathbf{M}|$  according to the time (noise level)  $t \in [0, 1]$ . The conditional distribution of the masked sequence  $x_t$  is defined as  $q_{t|0}(x_t|x_0) = \prod_{i=1}^L q_{t|0}(x_t^i|x_0^i)$ , where

$$q_{t|0}(x_t^i|x_0^i) = \begin{cases} 1 - t, & x_t^i = x_0^i, \\ t, & x_t^i = |\mathbf{M}|. \end{cases} \quad (1)$$

The reverse process aims to generate meaningful tokens from the all-masked sequence  $x_1$ . The conditional distribution is defined as  $q_{s|t}(x_s|x_t) = \prod_{i=1}^L q_{s|t}(x_s^i|x_t^i)$ , where  $0 \leq s < t \leq 1$ , and

$$q_{s|t}(x_s^i|x_t) = \begin{cases} 1, & x_s^i = x_t^i \neq |\mathbf{M}|, \\ \frac{s}{t}, & x_s^i = x_t^i = |\mathbf{M}|, \\ \frac{t-s}{t} q_{0|t}(x_s^i|x_t), & x_s^i \neq |\mathbf{M}|, x_t^i = |\mathbf{M}|, \\ 0, & \text{otherwise.} \end{cases} \quad (2)$$

A rigorous proof in [47] shows that  $q_{0|t}(x_s^i|x_t) = p(x_0^i|x_t^{\text{UM}})$ , where  $x_t^{\text{UM}}$  denotes the unmasked tokens in  $x_t$  that are identical to those in  $x_0$ . This implies that the time

condition  $t$  can be omitted from the model inputs, leading to a simplified implementation of MDLM in which the model only needs to predict masked tokens conditioned on the unmasked ones.

### 3.2. Tri-Level Cross-Modal Pretraining

Existing works [13, 71] reveal that the knowledge of LMs mainly comes from pretraining. As shown in Figure 2, we pretrain the MDLM at three spaces, enabling it to absorb knowledge from sign representations of different levels.

**Token Space.** At the first level, we pretrain the MDLM by predicting masked tokens. Following [45], at each training iteration, we uniformly sample a noise level (mask ratio)  $t \sim U(0, 1)$ . Denoting text tokens as  $x_e = \{x_e^i\}_{i=1}^{L_e}$  and an end-of-sentence token as  $|\text{eos}|$ , the input sequence is formed by concatenating text tokens,  $|\text{eos}|$ , and sign tokens:  $x_0 = \text{cat}(x_e, |\text{eos}|, x_{\{p\}}, |\text{eos}|) = \{x_0^i\}_{i=1}^{L_e+L_s+2}$ . For simplicity, we use  $\{p\}$  to denote all part-wise sign tokens, since they are masked and unmasked simultaneously once their index is selected. Each index  $i$  is selected with a probability of  $t$ , and its corresponding token is masked to obtain  $x_t$ . The token-space loss is defined as a cross-entropy loss [45]:

$$\mathcal{L}_{tok} = -\mathbb{E}_{t, x_0, x_t} \left[ \frac{1}{t} \sum_{i \in I_m} \log p_\theta(x_0^i | x_t) \right], \quad (3)$$

where  $I_m$  denote the set of masked indices, and  $p_\theta(\cdot)$  denotes the token probabilities predicted by the model.

**Latent Space.** Inspired by the effectiveness of predicting embeddings (features), *e.g.*, joint-embedding predictive architectures (JEPAs) [2, 36], in numerous vision tasks [3, 6, 93], we extend this idea to MDLM pretraining. In contrast to the original JEPAs that train an additional target encoder to extract features, we directly leverage the well-trained codebooks  $\mathcal{C}_p$ , whose code embeddings are natural sign representations, as the targets. More specifically, let the last hidden states of the MDLM corresponding to masked sign tokens be  $\mathbf{H} \in \mathbb{R}^{|I_s| \times d}$ , where  $I_s$  denotes the index set of masked sign tokens. We use three MLPs to map  $\mathbf{H}$  into the spaces of the codebooks:  $\mathbf{H}_p = \text{MLP}_p(\mathbf{H}) \in \mathbb{R}^{|I_s| \times d_c}$ , where  $d_c$  denotes the dimension of each code embedding. The target embeddings are then collected from the corresponding code embeddings:  $\hat{\mathbf{H}}_p = \text{cat}(\{\mathbf{c}_p^{n_i} | i \in I_s, 1 \leq n_i \leq N_c\})$ , where  $n_i$  denotes the code index of the  $i$ -th token. Finally, the MDLM learns to predict the code embeddings with a smoothed L1 loss:

$$\mathcal{L}_{lat} = \sum_p \text{Smooth\_L1}(\mathbf{H}_p, \hat{\mathbf{H}}_p). \quad (4)$$

**Physical Space.** Inspired by the visual–language nature of sign languages, we incorporate 3D sign motion reconstruction as an additional pretraining objective in the physical space. More specifically, we reuse the well-trained VAE

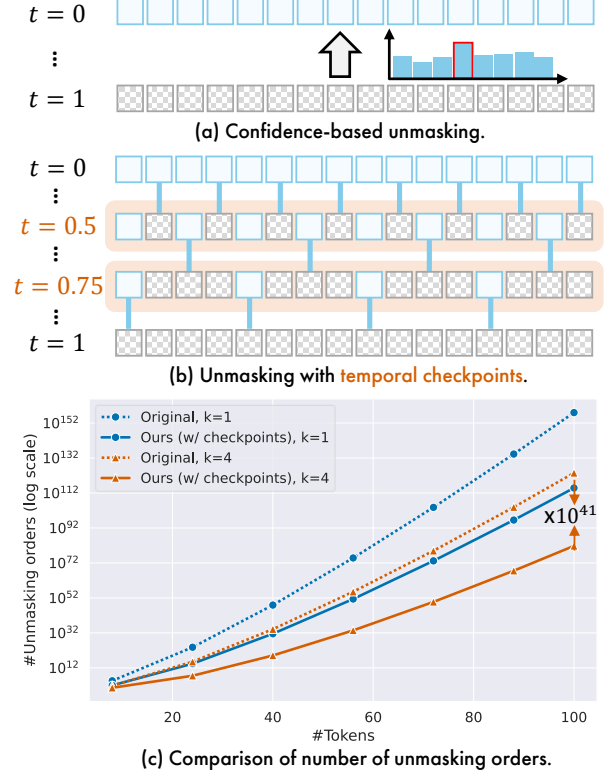


Figure 3. (a) Vanilla MDLMs adopt an unconstrained confidence-based unmasking strategy [45]. (b) We insert temporal checkpoints at noise levels 0.75 and 0.5 to reduce the complexity of unmasking orders. (c) The original unmasking strategy allows arbitrary unmasking orders (about  $10^{123}$  for generating 100 tokens), while our method reduces this complexity by over  $10^{41}$  times.

decoder  $\mathcal{D}_p$ , which is frozen and used to reconstruct sign motions from the mapped hidden states  $\mathbf{H}_p$ . Denoting the ground-truth part-wise sign motions at the masked indices as  $\hat{\mathbf{S}}_p$ , the objective function in the physical space is defined as:

$$\mathcal{L}_{phy} = \sum_p \text{Smooth\_L1}(\mathcal{D}_p(\mathbf{H}_p), \hat{\mathbf{S}}_p). \quad (5)$$

Unlike existing works [29, 57, 95] that mask and reconstruct sign poses, we mask tokens but reconstruct poses (motions), which is more challenging and encourages the model to learn more grounded sign representations. The overall pre-training loss is defined as  $\mathcal{L}_{pre} = \mathcal{L}_{tok} + \mathcal{L}_{lat} + \mathcal{L}_{phy}$ .

### 3.3. Supervised Fine-Tuning

After the pretraining stage, the MDLM is expected to acquire basic sign language knowledge and adapt to the diffusion process with bidirectional contexts. We then fine-tune the entire model while keeping the text tokens unmasked.

#### 3.3.1. Unmasking with Temporal Checkpoints (UTC)

During the reverse process, the original MDLM [45] adopts a simple confidence-based unmasking strategy (Figure 3a).

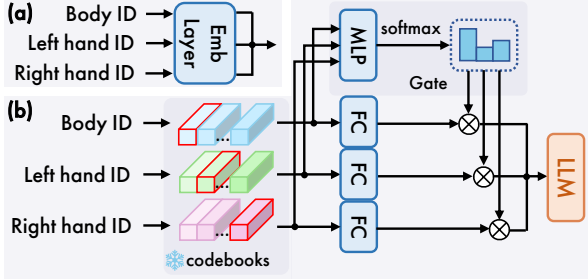


Figure 4. (a) A typical sign embedding layer averages part-wise token embeddings [98]. (b) The proposed mixture-of-parts embedding layer leverages optimized VAE codebooks and uses a learnable gate to control contributions from different body parts.

Specifically, at each step, the model unmasks  $k$  tokens with the highest confidence, defined as the maximum of their categorical probabilities. However, this unconstrained strategy leads to highly diverse unmasking orders. Denoting the number of generated tokens as  $M$ , the total number of possible unmasking orders is:

$$N_u = \binom{M}{k} \binom{M-k}{k} \cdots \binom{k}{k} = \frac{M!}{(k!)^{M/k}}. \quad (6)$$

When  $M = 100$  and  $k = 4$ , this number is approximately  $2.9 \times 10^{123}$ . Although such diversity can enhance model performance, it also results in slow convergence [52].

Inspired by VAR [70], which adopts a coarse-to-fine generation scheme with progressively enhanced resolution, we propose a novel unmasking strategy with temporal checkpoints (UTC), as shown in Figure 3b. Specifically, we divide the reverse process into three stages at  $t = 0.75$  and  $t = 0.5$ , where  $1/4$  and  $1/2$  of the tokens have been unmasked, respectively. Both pivot states are enforced to contain uniformly distributed tokens, while a standard confidence-based unmasking strategy is applied within each stage. Consequently, the number of possible orders under our UTC is substantially reduced to:

$$N_u^{\text{UTC}} = \frac{(M/4)!}{(k!)^{M/4k}} \cdot \frac{(M/4)!}{(k!)^{M/4k}} \cdot \frac{(M/2)!}{(k!)^{M/2k}}. \quad (7)$$

When  $M = 100$  and  $k = 4$ , UTC reduces the number of orders by  $10^{41} \times$  compared to vanilla unmasking strategy (Figure 3c), thereby improving training efficiency. Moreover, the model can generate coarse-grained results at lower temporal resolutions in the early stages of inference, which provides a basis for further acceleration. To ensure training–inference consistency, we employ predefined index masks to filter out infeasible states during training. More implementation details are provided in the supplement.

### 3.3.2. Mixture-of-Parts (MoP) Embedding Layer

In contrast to the pretraining stage, where different part-wise tokens are treated equally, we aim to more discrimi-

natively capture the relations among body parts during fine-tuning with text conditions. To this end, our MoP embedding layer is built upon the well-trained VAE codebooks and employs a learnable gate to control the contributions from different parts. For instance, since numerous signs are produced with a single hand [7, 22], it would be beneficial for the model to assign distinct weights to each hand.

As shown in Figure 4b, given the part IDs ( $i_p$ ), the part-wise code embeddings are passed through fully-connected (FC) layers to match the model dimension of MDLM:  $\mathbf{E}_p = \text{FC}_p(\mathbf{c}_p^{i_p})$ . Furthermore, we use an MLP with a softmax layer to learn gating weights:  $\mathbf{G} = \{g_p\} = \text{softmax}(\text{MLP}(\text{cat}(\{\mathbf{c}_p^{i_p}\})))$ . The final sign embedding is obtained as  $\mathbf{E} = \sum_p g_p \cdot \mathbf{E}_p$ .

Similar to [34], we also observe that continuing to use pretraining objectives during fine-tuning is beneficial. Therefore, the fine-tuning loss is defined as  $\mathcal{L}_{\text{soft}} = \mathcal{L}_{\text{tok}} + \alpha(\mathcal{L}_{\text{lat}} + \mathcal{L}_{\text{phy}})$ , where  $\alpha = 0.5$  by default.

## 3.4. SiBLEU and SiCLIP

Existing SLG models [1, 5, 96, 98] are typically evaluated using dynamic time warping (DTW) error [1] and back-translation (BT) [59]. However, DTW error may over-optimistically reflect model performance since it measures the minimum distance between generated and ground-truth sequences. Moreover, its computation is inefficient due to the reliance on dynamic programming. On the other hand, BT evaluates performance in the text space, which overlooks the visual and multi-cue nature of sign language, and the translation process itself introduces unavoidable errors [30]. To address these issues, we propose two new metrics that serve as effective alternatives.

**SiBLEU – Straightforward and Efficient Evaluation.** For LM-based SLG approaches, signs are tokenized, which enables a straightforward evaluation by computing BLEU scores [48] over generated tokens against ground-truth tokens. We term this the SiBLEU score. A higher SiBLEU indicates greater overlap with the ground truth.

**SiCLIP – Evaluation in a Joint Embedding Space.** In related domains such as human motion generation [42, 69] and text-to-video generation [78, 80, 89], CLIP [55] is widely used to evaluate the alignment between prompts (texts) and generations in a joint-embedding space. Motivated by this, we train a CLIP model over ground-truth sign-text pairs, and adopt retrieval-based metrics [8, 33, 50] for evaluating the semantic alignment between texts and generated signs. More details are provided in the supplement.

## 4. Experiments

**Datasets.** We evaluate MaDiS on three widely-adopted datasets: CSL-Daily [94], Phoenix-2014T [11], and How2Sign [18], which contain 20K/8K/35K video-text pairs for Chinese, American, and German sign languages,



Figure 5. Qualitative comparisons of generated signs between our proposed method, MaDiS, with the SOTA method, SOKE [98], on the test sets of CSL-Daily (left), Phoenix-2014T (middle), and How2Sign (right).

respectively. Since we focus on generating sign motions, we use the curated SMPL-X poses provided in [98].

**Evaluation Metrics.** Due to the length difference between generated signs and ground truth, we follow the previous work [98] to use dynamic time warping over joint position errors (DTW-JPE) as the major metric to measure sequence-level distances. Note that we do not compute procrustes alignment since it will align rotation before computing joint errors, leading to overoptimistic performance [9]. As a complement, we use SiBLEU-4 as an indicator for token-level precision and report the sentence-level sign-to-text retrieval performance ( $R@1$ ) [8, 16] using SiCLIP as a joint feature extractor for sign motions and texts.

**Implementation Details.** We instantiate the MDLM with Qwen3-0.6B-Base [81], a leading open-source LLM supporting 119 languages. To enable bidirectional modeling, we replace the causal attention mask in each transformer layer with a non-causal one [45]. During pretraining, the model is trained on the combined training sets of all three datasets to maximize data utilization [29]. In the fine-tuning

stage, it is trained on each dataset independently. We empirically set  $k = 4$  and  $M = 100$ , which corresponds to 400 frames after decoding due to the 4x up-sampling layer in the VAE decoder. This length is sufficient to cover about 98% of training videos, and over-length videos are uniformly sampled to fit within 400 frames. When generating sign tokens, we adopt multi-head decoding [98] to predict all three part-wise tokens simultaneously, and tokens appearing after the end-of-sentence token are discarded [45]. The initial learning rate is set to  $2e-4$ , and we adopt the AdamW optimizer [39] with a cosine learning rate scheduler and a batch size of 64 per GPU for both stages. The models are trained for 200 and 150 epochs in the pretraining and fine-tuning stages, respectively, using 4x Nvidia GH200 GPUs.

#### 4.1. Comparison with State-of-the-Art Methods

**Qualitative Comparison.** We first conduct qualitative comparisons with the previous SOTA method, SOKE [98], which proposes a simple autoregressive SLG model without dedicated pretraining and can only capture unidirec-

Method	CSL-Daily				Phoenix-2014T				How2Sign									
	DTW-JPE↓		SiBLEU↑		SiCLIP↑		DTW-JPE↓		SiBLEU↑		SiCLIP↑		DTW-JPE↓		SiBLEU↑		SiCLIP↑	
	Body	Hands	Body	Hands	R@1	Body	Hands	Body	Hands	R@1	Body	Hands	Body	Hands	R@1	Body	Hands	R@1
Prog. Trans.* [59]	16.30	32.63	N/A		13.65	15.01	31.77	N/A		14.03	14.74	30.17	N/A		9.88			
Text2Mesh* [66]	13.76	30.37	N/A		15.84	14.04	31.64	N/A		12.08	15.50	32.97	N/A		9.30			
T2S-GPT* [84]	12.32	15.43	2.11	N/A	20.03	11.65	19.09	1.93	N/A	22.10	12.65	18.44	2.13	N/A	12.58			
NSA [5]	—	—	N/A		—	—	—	N/A		—	9.16	18.51	N/A		15.04			
S-MotionGPT* [32]	11.58	11.31	2.26	N/A	20.37	10.42	9.08	1.97	N/A	32.42	12.41	13.74	2.32	N/A	12.77			
MoMask++ [27]	8.93	10.57	1.53	N/A	22.62	8.16	9.96	1.49	N/A	37.88	9.06	11.34	1.58	N/A	20.39			
SOKE (mBART) <sup>†</sup> [98]	7.38	9.68	2.59	2.14	23.64	6.04	7.72	2.71	1.85	34.30	7.75	10.08	2.52	1.74	16.12			
SOKE (Qwen3) <sup>†</sup> [98]	7.29	9.59	2.71	2.27	25.05	6.09	7.65	2.38	1.98	38.53	7.18	10.09	2.57	1.97	18.48			
MDLM baseline	7.12	9.57	3.17	2.55	29.17	5.98	7.58	2.36	2.14	44.25	7.02	10.16	2.73	1.79	25.78			
MaDiS (ours)	<b>5.99</b>	<b>7.96</b>	<b>4.87</b>	<b>4.08</b>	<b>38.61</b>	<b>4.97</b>	<b>6.59</b>	<b>4.54</b>	<b>3.33</b>	<b>57.94</b>	<b>6.59</b>	<b>9.45</b>	<b>4.41</b>	<b>3.46</b>	<b>34.27</b>			

Table 1. Comparison with SOTA sign language generation methods. Note that since SiBLEU scores are computed over sign tokens, we report ‘‘N/A’’ for tokenizer-free methods [5, 59, 66]. Similarly, for methods [27, 32, 84] that employ a single tokenizer for whole-body motions, the SiBLEU-hands results are also marked as ‘‘N/A’’. \*DTW errors are reported by [98]. <sup>†</sup>Methods using external sign dictionaries.

Method	CSL-Daily	Phoenix-2014T	How2Sign
SOKE [98]	1.074	1.019	1.021
MDLM baseline	0.784	0.723	0.735
MaDiS (ours)	0.782	0.724	0.734

Table 2. Comparison of inference latency (s/video) with SOKE. The generated sequence length is fixed at 100 tokens. All measurements are conducted on a single GH200 GPU.

tional contexts due to the nature of ARLMs. In contrast, our MaDiS is pretrained across multiple sign representation spaces and benefits from an MDLM backbone that enables bidirectional contextual modeling. As shown in Figure 5, our model produces more precise and natural sign motions, demonstrating better generalization across diverse hand shapes, palm orientations, single- and double-handed signs, and finger details.

**Quantitative Comparison.** As detailed in Table 1, we conduct a quantitative comparison with SOTA SLG methods. Since we introduce two new evaluation metrics, we carefully reproduce previous works using their open-source codes [27, 32, 59, 66, 98] or our own reimplementations [5, 84]. MoMask++ [27] is a leading human motion generation method based on a masked generation approach [12]. However, its masking schedule is heuristically determined without a theoretical foundation, and its multi-scale tokenization introduces error accumulation during inference, leading to inferior performance than SOKE. For fairness, we also report the performance of SOKE when using Qwen3-0.6B as the LM, instead of the originally adopted mBART-Large [38]. We observe that employing Qwen3 leads to slightly better performance, which can be attributed to the larger pretraining corpus of the Qwen3 series. Furthermore, we report the performance of an MDLM baseline, obtained by directly training an MDLM on sign language datasets. Notably, even without any pretraining techniques, this baseline performs on par with SOKE, which

Token	Latent	Physical	DTW-JPE↓	SiBLEU↑	SiCLIP↑
			Body	Hands	Body
Sign	Text		6.93	9.27	3.48
✓			6.81	8.90	3.76
✓	✓		6.41	8.64	4.18
✓	✓	✓	6.22	8.39	4.45
✓	✓	✓	<b>5.99</b>	<b>7.96</b>	<b>4.87</b>
		✓			3.67
		✓			35.96
		✓			<b>38.61</b>

Table 3. Ablation study for the tri-level cross-modal pretraining.

utilizes external sign dictionaries, while offering reduced latency (Table 2). This highlights the potential of masked diffusion language models for SLG. Finally, our proposed MaDiS achieves new SOTA results across the test sets of all three datasets and all evaluation metrics.

**Efficiency.** Real-world applications typically demand low-latency systems. We evaluate the inference latency of our model against previous ARLM-based SLG method, SOKE, as reported in Table 2. Across the three datasets, our method consistently achieves around 30% reduction in latency, attributable to the highly efficient parallel token generation enabled by the reverse process in MDLMs.

## 4.2. Ablation Studies

We conduct all ablation studies on CSL-Daily.

**Tri-Level Cross-Modal Pretraining.** We pretrain the model across three spaces (token, latent, and physical) to enable it to learn rich sign representations at different levels. Results in Table 3 validate the effectiveness of each pretraining level. First, at the token level, masking both sign and text tokens yields better performance than masking sign tokens alone, demonstrating the benefit of cross-modal training. This observation is consistent with previous findings on alignment-based pretraining in sign language translation [34, 40, 92]. Second, predicting latent features proves effective in reducing DTW errors and enhancing sentence-level semantic alignment. Finally, incorporating physical-

Checkpoint	DTW-JPE↓		SiBLEU↑		SiCLIP↑	
	Body	Hands	Body	Hands	R@1	
$t = 0.75$	6.61	9.05	3.87	3.11	32.81	
$t = 0.5$	6.33	8.73	4.15	3.52	34.09	
$t = 0.75/0.5$	6.18	8.23	4.63	3.94	36.73	
<b><math>t = 0.75/0.5</math></b>	<b>5.99</b>	<b>7.96</b>	<b>4.87</b>	<b>4.08</b>	<b>38.61</b>	

Table 4. Ablation study for unmasking with temporal checkpoints.

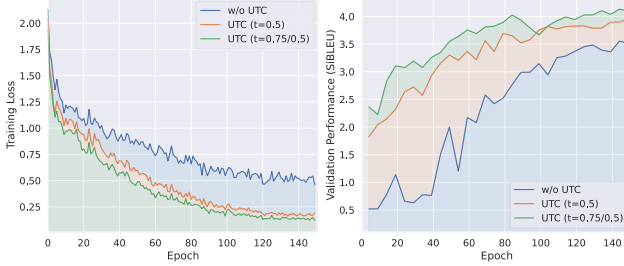


Figure 6. Visualization of training loss (left) and validation performance (average of SiBLEU-body and SiBLEU-hands, right).

space training by reconstructing sign motions leads to the best overall performance.

**Unmasking with Temporal Checkpoints (UTC).** To accelerate model convergence, we propose a novel unmasking strategy with temporal checkpoints, which substantially reduces the complexity of unmasking orders. As shown in Table 4, inserting checkpoints at either  $t = 0.75$  (corresponding to a  $T/4$  temporal resolution) or  $t = 0.5$  ( $T/2$  temporal resolution) yields superior performance compared to the no-checkpoint baseline. The best results are achieved when both checkpoints are applied. Furthermore, to examine whether the proposed UTC effectively accelerates training convergence, we visualize the training loss ( $\mathcal{L}_{tok}$ ) and validation performance in Figure 6. The curves clearly demonstrate that incorporating checkpoints leads to faster convergence, which is reflected by lower training loss and higher validation performance at the same epoch.

**Mixture-of-Parts (MoP) Embedding Layer.** Our MoP sign embedding layer is built upon a dense mixture-of-experts (MoE) mechanism [10], in which all experts (body parts) are activated but controlled by a learnable gate. As shown in Table 5, we compare this design with a sparse MoE variant that fuses only the body parts corresponding to the top-1 or top-2 activation values. We observe that this sparse configuration results in inferior performance compared to the default dense setting. In Figure 7, we further visualize the learned gating weights for four example signs. For single-handed signs (left two examples), our MoP layer assigns higher weights to the active hand, indicating that it effectively captures hand dominance. In contrast, for two-handed signs, the layer learns comparable weights for both hands, reflecting balanced contributions during generation.

**SiCLIP.** To better evaluate the semantic alignment between

Method	DTW-JPE↓		SiBLEU↑		SiCLIP↑	
	Body	Hands	Body	Hands	R@1	
Simple Avg [98]	6.35	8.50	4.06	3.42	35.95	
Sparse MoE (Top-1)	6.48	8.74	3.76	3.27	35.65	
Sparse MoE (Top-2)	6.29	8.41	3.91	3.50	36.87	
Dense MoE (ours)	<b>5.99</b>	<b>7.96</b>	<b>4.87</b>	<b>4.08</b>	<b>38.61</b>	

Table 5. Ablation study for the MoP embedding layer.

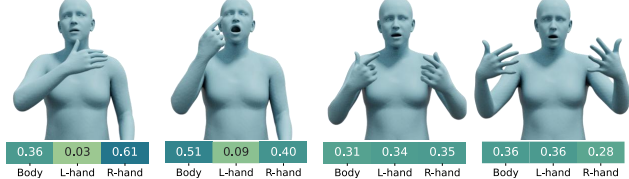


Figure 7. Visualization of the learned gating weights  $G$ .

Method	CSL-Daily↑		Phoenix↑		How2Sign↑	
	R@1	R@5	R@1	R@5	R@1	R@5
Baseline (CLIP) [33]	41.07	81.97	58.41	88.01	9.27	28.47
+ Decoupled encoders	45.07	85.88	61.84	90.03	12.13	38.48
+ Fine-grained loss	<b>59.10</b>	<b>95.66</b>	<b>68.85</b>	<b>95.64</b>	<b>41.33</b>	<b>88.43</b>

Table 6. Ablation study for the SiCLIP.

texts and generated signs, we follow established practices in related fields [42, 69] and train a CLIP model over ground-truth sign motions and texts, referred to as SiCLIP. We assess its performance using the sign-to-text retrieval task. As shown in Table 6, simply using a contrastive loss [33] results in low retrieval performance. Introducing decoupled sign encoders [98] yields noticeable improvements. Most of the gains come from the fine-grained contrastive loss [16], which implicitly learns precise word-level alignments. The final retrieval performance is on par with that of a leading motion retrieval model [50], validating the effectiveness of SiCLIP as a reliable evaluator for future SLG research.

## 5. Conclusion

We present MaDiS, a novel SLG approach built upon MDLMs that enable bidirectional context modeling and efficient generation. To effectively inject sign language knowledge into MDLMs, we design a tri-level cross-modal pretraining framework that jointly learns from token, latent, and 3D physical spaces. To improve training efficiency of MDLMs, we simplify unmasking orders by proposing a novel unmasking strategy with temporal checkpoints. Moreover, a mixture-of-parts sign embedding layer is introduced to enhance part-wise token integration through gated, codebook-conditioned fusion. Experiments on standard SLG benchmarks demonstrate that MaDiS achieves SOTA performance across multiple evaluation metrics, while reducing inference latency by nearly 30%.

**Acknowledgements.** S. Zafeiriou and part of the research was funded by the EPSRC Fellowship DEFORM (EP/S010203/1), EPSRC Project GNOMON (EP/X011364/1) and Turing AI Fellowship (EP/Z534699/1). R.A. Potamias and R. Zuo were supported by EPSRC Project GNOMON (EP/X011364/1). J. Deng was supported by the NVIDIA Academic Grant.

The authors acknowledge the use of resources provided by the Isambard-AI National AI Research Resource (AIRR). Isambard-AI [41] is operated by the University of Bristol and is funded by the UK Government’s Department for Science, Innovation and Technology (DSIT) via UK Research and Innovation; and the Science and Technology Facilities Council [ST/AIRR/I-A-I/1023].

## References

- [1] Rotem Shalev Arkushin, Amit Moryossef, and Ohad Fried. Ham2pose: Animating sign language notation into pose sequences. In *CVPR*, pages 21046–21056, 2023. [2](#), [5](#)
- [2] Mahmoud Assran, Quentin Duval, Ishan Misra, Piotr Bojanowski, Pascal Vincent, Michael Rabbat, Yann LeCun, and Nicolas Ballas. Self-supervised learning from images with a joint-embedding predictive architecture. In *CVPR*, 2023. [4](#)
- [3] Mido Assran, Adrien Bardes, David Fan, Quentin Garrido, Russell Howes, Matthew Muckley, Ammar Rizvi, Claire Roberts, Koustuv Sinha, Artem Zholus, et al. V-jepa 2: Self-supervised video models enable understanding, prediction and planning. *arXiv preprint arXiv:2506.09985*, 2025. [2](#), [4](#)
- [4] Federico Baldassarre, Marc Szafraniec, Basile Terver, Vasil Khalidov, Francisco Massa, Yann LeCun, Patrick Labatut, Maximilian Seitzer, and Piotr Bojanowski. Back to the features: Dino as a foundation for video world models. *arXiv preprint arXiv:2507.19468*, 2025. [2](#)
- [5] Vasileios Baltatzis, Rolandoz Alexandros Potamias, Evangelos Ververas, Guanxiong Sun, Jiankang Deng, and Stefanos Zafeiriou. Neural sign actors: A diffusion model for 3d sign language production from text. In *CVPR*, pages 1985–1995, 2024. [1](#), [5](#), [7](#)
- [6] Adrien Bardes, Quentin Garrido, Jean Ponce, Xinlei Chen, Michael Rabbat, Yann LeCun, Mahmoud Assran, and Nicolas Ballas. Revisiting feature prediction for learning visual representations from video. *TMLR*, 2024. [2](#), [4](#)
- [7] Robbin Battison. *Lexical borrowing in American sign language*. ERIC, 1978. [5](#)
- [8] Léore Bensabath, Mathis Petrovich, and Gü̈l Varol. Text-driven 3d hand motion generation from sign language data. *arXiv preprint arXiv:2508.15902*, 2025. [5](#), [6](#)
- [9] Michael J Black, Priyanka Patel, Joachim Tesch, and Jinlong Yang. Bedlam: A synthetic dataset of bodies exhibiting detailed lifelike animated motion. In *CVPR*, 2023. [6](#)
- [10] Weilin Cai, Juyong Jiang, Fan Wang, Jing Tang, Sunghun Kim, and Jiayi Huang. A survey on mixture of experts in large language models. *TKDE*, 2025. [8](#)
- [11] Necati Cihan Camgoz, Simon Hadfield, Oscar Koller, Hermann Ney, and Richard Bowden. Neural sign language translation. In *CVPR*, 2018. [1](#), [2](#), [5](#)
- [12] Huiwen Chang, Han Zhang, Lu Jiang, Ce Liu, and William T Freeman. Maskgit: Masked generative image transformer. In *CVPR*, 2022. [3](#), [7](#)
- [13] Hoyeon Chang, Jinho Park, Seonghyeon Ye, Sohee Yang, Youngkyung Seo, Du-Seong Chang, and Minjoon Seo. How do large language models acquire factual knowledge during pretraining? *NeurIPS*, 2024. [4](#)
- [14] Yutong Chen, Ronglai Zuo, Fangyun Wei, Yu Wu, Shujie Liu, and Brian Mak. Two-stream network for sign language recognition and translation. In *NeurIPS*, 2022. [1](#)
- [15] Zhigang Chen, Benjia Zhou, Yiqing Huang, Jun Wan, Yibo Hu, Hailin Shi, Yanyan Liang, Zhen Lei, and Du Zhang. C2rl: Content and context representation learning for gloss-free sign language translation and retrieval. *IEEE TCSV*, 2025. [3](#)
- [16] Yiting Cheng, Fangyun Wei, Jianmin Bao, Dong Chen, and Wenqiang Zhang. Cico: Domain-aware sign language retrieval via cross-lingual contrastive learning. In *CVPR*, 2023. [6](#), [8](#)
- [17] Lu Dong, Lipisha Chaudhary, Fei Xu, Xiao Wang, Mason Lary, and Ifeoma Nwogu. Signavator: Sign language 3d motion reconstruction and generation. In *FG*, 2024. [1](#), [2](#)
- [18] Amanda Duarte, Shruti Palaskar, Lucas Ventura, Deepti Ghadiyaram, Kenneth DeHaan, Florian Metze, Jordi Torres, and Xavier Giro-i Nieto. How2sign: a large-scale multimodal dataset for continuous american sign language. In *CVPR*, pages 2735–2744, 2021. [1](#), [2](#), [5](#)
- [19] Sen Fang, Chunyu Sui, Yanghao Zhou, Xuedong Zhang, Hongbin Zhong, Yapeng Tian, and Chen Chen. Signdiff: Diffusion model for american sign language production. In *FG*, 2025. [1](#)
- [20] Sen Fang, Lei Wang, Ce Zheng, Yapeng Tian, and Chen Chen. Signllm: Sign languages production large language models. In *ICCVW*, 2025. [1](#)
- [21] Edward Fish and Richard Bowden. Geo-sign: Hyperbolic contrastive regularisation for geometrically aware sign language translation. *NeurIPS*, 2025. [1](#)
- [22] Maria-Paola Forte, Peter Kulits, Chun-Hao P Huang, Vasileios Choutas, Dimitrios Tzionas, Katherine J Kuchenbecker, and Michael J Black. Reconstructing signing avatars from video using linguistic priors. In *CVPR*, pages 12791–12801, 2023. [5](#)
- [23] Jia Gong, Lin Geng Foo, Yixuan He, Hossein Rahmani, and Jun Liu. Llms are good sign language translators. In *CVPR*, pages 18362–18372, 2024. [1](#)
- [24] Shanshan Gong, Shivam Agarwal, Yizhe Zhang, Jiacheng Ye, Lin Zheng, Mukai Li, Chenxin An, Peilin Zhao, Wei Bi, Jiawei Han, et al. Scaling diffusion language models via adaptation from autoregressive models. In *ICLR*, 2025. [2](#)
- [25] Shester Gueuwou, Xiaodan Du, Greg Shakhnarovich, Karen Livescu, and Alexander H Liu. Shubert: Self-supervised sign language representation learning via multi-stream cluster prediction. In *ACL*, 2025. [3](#)

[26] Chuan Guo, Yuxuan Mu, Muhammad Gohar Javed, Sen Wang, and Li Cheng. Momask: Generative masked modeling of 3d human motions. In *CVPR*, pages 1900–1910, 2024. 3

[27] Chuan Guo, Inwoo Hwang, Jian Wang, and Bing Zhou. Snapmogen: Human motion generation from expressive texts. In *NeurIPS*, 2025. 3, 7

[28] Jianyuan Guo, Peike Li, and Trevor Cohn. Bridging sign and spoken languages: Pseudo gloss generation for sign language translation. *NeurIPS*, 2025. 1

[29] Hezhen Hu, Weichao Zhao, Wengang Zhou, and Houqiang Li. SignBERT+: Hand-model-aware self-supervised pre-training for sign language understanding. *TPAMI*, 2023. 2, 3, 4, 6

[30] Saki Imai, Mert İnan, Anthony Sicilia, and Malihe Alikhani. Silverscore: Semantically-aware embeddings for sign language generation evaluation. In *International Conference on Recent Advances in Natural Language Processing*, 2025. 5

[31] Youngjoon Jang, Haran Raajesh, Liliane Momeni, GÜl Varol, and Andrew Zisserman. Lost in translation, found in context: Sign language translation with contextual cues. In *CVPR*, 2025. 1

[32] Biao Jiang, Xin Chen, Wen Liu, Jingyi Yu, Gang Yu, and Tao Chen. Motiongpt: Human motion as a foreign language. *NeurIPS*, 36:20067–20079, 2023. 7

[33] Zifan Jiang, Gerard Sant, Amit Moryossef, Mathias Müller, Rico Sennrich, and Sarah Ebliing. Signclip: Connecting text and sign language by contrastive learning. In *EMNLP*, 2024. 5, 8

[34] Peiqi Jiao, Yuecong Min, and Xilin Chen. Visual alignment pre-training for sign language translation. In *ECCV*, pages 349–367, 2024. 2, 3, 5, 7

[35] Jungeun Kim, Hyeongwoo Jeon, Jongseong Bae, and Ha Young Kim. Leveraging the power of mllms for gloss-free sign language translation. In *ICCV*, 2025. 3

[36] Yann LeCun. A path towards autonomous machine intelligence. *Open Review*, 62(1):1–62, 2022. 2, 4

[37] Zecheng Li, Wengang Zhou, Weichao Zhao, Kepeng Wu, Hezhen Hu, and Houqiang Li. Uni-sign: Toward unified sign language understanding at scale. In *ICLR*, 2025. 1, 2, 3

[38] Yinhan Liu, Jiatao Gu, Naman Goyal, Xian Li, Sergey Edunov, Marjan Ghazvininejad, Mike Lewis, and Luke Zettlemoyer. Multilingual denoising pre-training for neural machine translation. *TACL*, 8:726–742, 2020. 7

[39] Ilya Loshchilov and Frank Hutter. Decoupled weight decay regularization. In *ICLR*, 2019. 6

[40] Jian He Low, Ozge Mercanoglu Sincan, and Richard Bowden. Sage: Segment-aware gloss-free encoding for token-efficient sign language translation. In *ICCVW*, 2025. 7

[41] Simon McIntosh-Smith, Sadaf Alam, and Christopher Woods. Isambard-ai: a leadership-class supercomputer optimised specifically for artificial intelligence. In *Proceedings of the Cray User Group*, pages 44–54. ACM, 2024. 9

[42] Zichong Meng, Yiming Xie, Xiaogang Peng, Zeyu Han, and Huaizu Jiang. Rethinking diffusion for text-driven human motion generation: Redundant representations, evaluation, and masked autoregression. In *CVPR*, 2025. 5, 8

[43] Shentong Mo and Shengbang Tong. Connecting joint-embedding predictive architecture with contrastive self-supervised learning. *NeurIPS*, 2024. 2

[44] Shen Nie, Fengqi Zhu, Chao Du, Tianyu Pang, Qian Liu, Guangtao Zeng, Min Lin, and Chongxuan Li. Scaling up masked diffusion models on text. In *ICLR*, 2025. 2, 3

[45] Shen Nie, Fengqi Zhu, Zebin You, Xiaolu Zhang, Jingyang Ou, Jun Hu, Jun Zhou, Yankai Lin, Ji-Rong Wen, and Chongxuan Li. Large language diffusion models. *NeurIPS*, 2025. 1, 2, 3, 4, 6

[46] Zhe Niu, Ronglai Zuo, Brian Mak, and Fangyun Wei. A Hong Kong sign language corpus collected from sign-interpreted tv news. In *LREC-COLING*, pages 636–646, 2024. 1

[47] Jingyang Ou, Shen Nie, Kaiwen Xue, Fengqi Zhu, Jiacheng Sun, Zhenguo Li, and Chongxuan Li. Your absorbing discrete diffusion secretly models the conditional distributions of clean data. *ICLR*, 2025. 2, 3

[48] Kishore Papineni, Salim Roukos, Todd Ward, and Wei-Jing Zhu. BLEU: a method for automatic evaluation of machine translation. In *ACL*, pages 311–318, 2002. 5

[49] Georgios Pavlakos, Vasileios Choutas, Nima Ghorbani, Timo Bolkart, Ahmed AA Osman, Dimitrios Tzionas, and Michael J Black. Expressive body capture: 3D hands, face, and body from a single image. In *CVPR*, pages 10975–10985, 2019. 3

[50] Mathis Petrovich, Michael J Black, and GÜl Varol. Tmr: Text-to-motion retrieval using contrastive 3d human motion synthesis. In *ICCV*, pages 9488–9497, 2023. 5, 8

[51] Ekkasit Pinyoanuntapong, Muhammad Saleem, Korrawe Karunratanakul, Pu Wang, Hongfei Xue, Chen Chen, Chuan Guo, Junli Cao, Jian Ren, and Sergey Tulyakov. Maskcontrol: Spatio-temporal control for masked motion synthesis. In *ICCV*, 2025. 3

[52] Mihir Prabhudesai, Mengning Wu, Amir Zadeh, Katerina Fragkiadaki, and Deepak Pathak. Diffusion beats autoregressive in data-constrained settings. *NeurIPS*, 2025. 2, 3, 5

[53] Fan Qi, Yu Duan, Changsheng Xu, and Huaiwen Zhang. Signgen: End-to-end sign language video generation with latent diffusion. In *ECCV*, 2024. 2

[54] Guanren Qiao, Sixu Lin, Ronglai Zuo, Zhizheng Wu, Kui Jia, and Guiliang Liu. Signbot: Learning human-to-humanoid sign language interaction. *arXiv preprint arXiv:2505.24266*, 2025. 2

[55] Alec Radford, Jong Wook Kim, Chris Hallacy, Aditya Ramesh, Gabriel Goh, Sandhini Agarwal, Girish Sastry, Amanda Askell, Pamela Mishkin, Jack Clark, et al. Learning transferable visual models from natural language supervision. In *ICML*, pages 8748–8763, 2021. 5

[56] Robin Rombach, Andreas Blattmann, Dominik Lorenz, Patrick Esser, and Björn Ommer. High-resolution image synthesis with latent diffusion models. In *CVPR*, pages 10684–10695, 2022. 1

[57] Phillip Rust, Bowen Shi, Skyler Wang, Necati Cihan Camgoz, and Jean Maillard. Towards privacy-aware sign language translation at scale. In *ACL*, pages 8624–8641, 2024. 3, 4

[58] Subham Sahoo, Marianne Arriola, Yair Schiff, Aaron Gokaslan, Edgar Marroquin, Justin Chiu, Alexander Rush, and Volodymyr Kuleshov. Simple and effective masked diffusion language models. *NeurIPS*, 2024. 2

[59] Ben Saunders, Necati Cihan Camgoz, and Richard Bowden. Progressive transformers for end-to-end sign language production. In *ECCV*, pages 687–705, 2020. 5, 7

[60] Ben Saunders, Necati Cihan Camgoz, and Richard Bowden. Mixed signals: Sign language production via a mixture of motion primitives. In *ICCV*, pages 1919–1929, 2021. 2

[61] Ben Saunders, Necati Cihan Camgoz, and Richard Bowden. Signing at scale: Learning to co-articulate signs for large-scale photo-realistic sign language production. In *CVPR*, pages 5141–5151, 2022. 1, 2

[62] Jiaxin Shi, Kehang Han, Zhe Wang, Arnaud Doucet, and Michalis Titsias. Simplified and generalized masked diffusion for discrete data. *NeurIPS*, 2024. 2

[63] Tongkai Shi, Lianyu Hu, Fanhua Shang, Jichao Feng, Peidong Liu, and Wei Feng. Pose-guided fine-grained sign language video generation. In *ECCV*, pages 392–409, 2024. 2

[64] Tongkai Shi, Lianyu Hu, Fanhua Shang, Liqing Gao, and Wei Feng. Greg: Geometry-aware region refinement for sign language video generation. In *ICCV*, 2025. 1, 2

[65] Yuxuan Song, Zheng Zhang, Cheng Luo, Pengyang Gao, Fan Xia, Hao Luo, Zheng Li, Yuehang Yang, Hongli Yu, Xingwei Qu, et al. Seed diffusion: A large-scale diffusion language model with high-speed inference. *arXiv preprint arXiv:2508.02193*, 2025. 2

[66] Stephanie Stoll, Armin Mustafa, and Jean-Yves Guillemaut. There and back again: 3d sign language generation from text using back-translation. In *3DV*, pages 187–196, 2022. 7

[67] Shengeng Tang, Richang Hong, Dan Guo, and Meng Wang. Gloss semantic-enhanced network with online back-translation for sign language production. In *MM*, pages 5630–5638, 2022. 2

[68] Shengeng Tang, Jiayi He, Lechao Cheng, Jingjing Wu, Dan Guo, and Richang Hong. Discrete to continuous: Generating smooth transition poses from sign language observations. In *CVPR*, 2025. 1, 2

[69] Guy Tevet, Brian Gordon, Amir Hertz, Amit H Bermano, and Daniel Cohen-Or. Motionclip: Exposing human motion generation to clip space. In *ECCV*, 2022. 5, 8

[70] Keyu Tian, Yi Jiang, Zehuan Yuan, Bingyue Peng, and Liwei Wang. Visual autoregressive modeling: Scalable image generation via next-scale prediction. *NeurIPS*, 2024. 2, 5

[71] Kushal Tirumala, Aram Markosyan, Luke Zettlemoyer, and Armen Aghajanyan. Memorization without overfitting: Analyzing the training dynamics of large language models. *NeurIPS*, 2022. 4

[72] Aaron Van Den Oord, Oriol Vinyals, et al. Neural discrete representation learning. *NeurIPS*, 30, 2017. 3

[73] Cong Wang, Zexuan Deng, Zhiwei Jiang, Fei Shen, Yafeng Yin, Shiwei Gan, Zifeng Cheng, Shiping Ge, and Qing Gu. Advanced sign language video generation with compressed and quantized multi-condition tokenization. In *NeurIPS*, 2025. 1, 2

[74] Xinyou Wang, Zaixiang Zheng, Fei Ye, Dongyu Xue, Shujian Huang, and Quanquan Gu. Diffusion language models are versatile protein learners. In *ICML*, 2024. 3

[75] Yuqing Wen, Hebei Li, Kefan Gu, Yucheng Zhao, Tiancai Wang, and Xiaoyan Sun. Llada-vla: Vision language diffusion action models. *arXiv preprint arXiv:2509.06932*, 2025. 3

[76] Ryan Wong, Necati Cihan Camgoz, and Richard Bowden. Sign2gpt: Leveraging large language models for gloss-free sign language translation. In *ICLR*, 2024. 1

[77] Ryan Wong, Necati Cihan Camgoz, and Richard Bowden. Signrep: Enhancing self-supervised sign representations. In *ICCV*, 2025. 2, 3

[78] Jay Zhangjie Wu, Yixiao Ge, Xintao Wang, Stan Weixian Lei, Yuchao Gu, Yufei Shi, Wynne Hsu, Ying Shan, Xiaohu Qie, and Mike Zheng Shou. Tune-a-video: One-shot tuning of image diffusion models for text-to-video generation. In *ICCV*, 2023. 5

[79] Pan Xie, Qipeng Zhang, Peng Taiying, Hao Tang, Yao Du, and Zexian Li. G2p-ddm: Generating sign pose sequence from gloss sequence with discrete diffusion model. In *AAAI*, pages 6234–6242, 2024. 2

[80] Zhen Xing, Qi Dai, Han Hu, Zuxuan Wu, and Yu-Gang Jiang. Simda: Simple diffusion adapter for efficient video generation. In *CVPR*, 2024. 5

[81] An Yang, Anfeng Li, Baosong Yang, Beichen Zhang, Binyuan Hui, Bo Zheng, Bowen Yu, Chang Gao, Chengan Huang, Chenxu Lv, et al. Qwen3 technical report. *arXiv preprint arXiv:2505.09388*, 2025. 6

[82] Ling Yang, Ye Tian, Bowen Li, Xinchen Zhang, Ke Shen, Yunhai Tong, and Mengdi Wang. Mmada: Multimodal large diffusion language models. In *NeurIPS*, 2025. 2, 3

[83] Jinhui Ye, Xing Wang, Wenxiang Jiao, Junwei Liang, and Hui Xiong. Improving gloss-free sign language translation by reducing representation density. *NeurIPS*, 2024. 3

[84] Aoxiong Yin, Haoyuan Li, Kai Shen, Siliang Tang, and Yueteng Zhuang. T2S-GPT: Dynamic vector quantization for autoregressive sign language production from text. In *ACL*, 2024. 1, 2, 7

[85] Kayo Yin, Amit Moryossef, Julie Hochgesang, Yoav Goldberg, and Malihe Alikhani. Including signed languages in natural language processing. In *ACL*, pages 7347–7360, 2021. 1

[86] Zebin You, Shen Nie, Xiaolu Zhang, Jun Hu, Jun Zhou, Zhiwu Lu, Ji-Rong Wen, and Chongxuan Li. Llada-v: Large language diffusion models with visual instruction tuning. *arXiv preprint arXiv:2505.16933*, 2025. 2

[87] Zhengdi Yu, Shaoli Huang, Yongkang Cheng, and Tolga Birdal. Signavatars: A large-scale 3d sign language holistic motion dataset and benchmark. In *ECCV*, pages 1–19, 2024. 1, 2

[88] Biao Zhang, Garrett Tanzer, and Orhan Firat. Scaling sign language translation. *NeurIPS*, 2024. 3

[89] Yabo Zhang, Yuxiang Wei, Dongsheng Jiang, Xiaopeng Zhang, Wangmeng Zuo, and Qi Tian. Controlvideo: Training-free controllable text-to-video generation. In *ICLR*, 2024. 5

- [90] Weichao Zhao, Hezhen Hu, Wengang Zhou, Jiaxin Shi, and Houqiang Li. BEST: BERT pre-training for sign language recognition with coupling tokenization. In *AAAI*, 2023. 3
- [91] Weichao Zhao, Hezhen Hu, Wengang Zhou, Yunyao Mao, Min Wang, and Houqiang Li. Masa: Motion-aware masked autoencoder with semantic alignment for sign language recognition. *IEEE TCSVT*, 2024. 3
- [92] Benjia Zhou, Zhigang Chen, Albert Clapés, Jun Wan, Yanyan Liang, Sergio Escalera, Zhen Lei, and Du Zhang. Gloss-free sign language translation: Improving from visual-language pretraining. In *ICCV*, pages 20871–20881, 2023. 2, 3, 7
- [93] Gaoyue Zhou, Hengkai Pan, Yann LeCun, and Lerrel Pinto. Dino-wm: World models on pre-trained visual features enable zero-shot planning. In *ICML*, 2025. 2, 4
- [94] Hao Zhou, Wengang Zhou, Weizhen Qi, Junfu Pu, and Houqiang Li. Improving sign language translation with monolingual data by sign back-translation. In *CVPR*, 2021. 1, 2, 5
- [95] Wengang Zhou, Weichao Zhao, Hezhen Hu, Zecheng Li, and Houqiang Li. Scaling up multimodal pre-training for sign language understanding. *TPAMI*, 2025. 2, 3, 4
- [96] Ronglai Zuo, Fangyun Wei, Zenggui Chen, Brian Mak, Jiaolong Yang, and Xin Tong. A simple baseline for spoken language to sign language translation with 3d avatars. In *ECCV*, 2024. 2, 5
- [97] Ronglai Zuo, Fangyun Wei, and Brian Mak. Towards online continuous sign language recognition and translation. In *EMNLP*, 2024. 1
- [98] Ronglai Zuo, Rolandos Alexandros Potamias, Evangelos Ververas, Jiankang Deng, and Stefanos Zafeiriou. Signs as tokens: A retrieval-enhanced multilingual sign language generator. In *ICCV*, 2025. 1, 2, 3, 5, 6, 7, 8